

**Dynamic Protein Adsorption in Microchannels by “Stop-Flow” and Continuous Flow.
Supporting Information (SI).**

*Andrea Lionello, Jacques Josserand, Henrik Jensen, Hubert H. Girault**

Laboratoire d'Electrochimie Physique et Analytique, Institut des Sciences et Ingénierie
Chimiques (ISIC),
Ecole Polytechnique Fédérale de Lausanne, CH-1015 Lausanne, Switzerland

*Corresponding author: (e-mail) hubert.girault@epfl.ch; (phone) + 41 693 31 51; (fax) + 41 21
693 36 67.

SI Index

page S-2 - General forms of the equations of the model (Galerkin formulation).

page S-4 - Numerical technique.

page S-5 - Effects of the velocity profile, diffusion coefficient and channel length on the adsorption.

page S-7 - Time comparison between continuous flow and “stop-flow” in a diffusion limited case.

page S-10 – Figures.

Theory

General form of the equations of the model (Galerkin formulation).

The evolution of C and Γ in the present FEM model is calculated by the following set of equations, which are applied to the 2-D geometry described in Fig. S11. Note that the boundary condition (9 - paper) is introduced in (8 - paper) as a consumption term assigned to the active wall, leading to eq. (SI1). To ensure that the adsorption term is only applied on the wall region for both eq. (SI1-2) and (SI5-6), the surface concentration Γ' , and the kinetic rates k_{on} and k_{off} are defined only at the wall surface; C is defined both in the bulk and at the wall. The second terms of eq. (SI2) and (SI1) equal zero in the bulk. The present model has been calibrated with previous numerical results^{1,2} for the Langmuir adsorption isotherm.³

$$\frac{\partial C}{\partial t} + \nabla \cdot (-D \nabla C + V C) = -k_{\text{on}} C (\Gamma'_{\text{max}} - \Gamma') + k_{\text{off}} \Gamma' \quad (\text{SI1})$$

$$\frac{\partial \Gamma'}{\partial t} + \nabla \cdot (-D_{\text{wall}} \nabla \Gamma') = k_{\text{on}} C (\Gamma'_{\text{max}} - \Gamma') - k_{\text{off}} \Gamma' \quad (\text{SI2})$$

The notation $\Gamma' = \Gamma/\delta$ is here introduced to render dimensionally homogeneous the two sides of eq. (SI1) and (SI2), δ representing the arbitrary thickness of the active wall (see Fig. S11) to eventually study adsorption in thin layers (note that $\delta/h = 0.04$). Because of the introduction of δ , the sorbent surface cross section is not linear but 2-dimensional: Γ' is in $\text{mol}\cdot\text{m}^{-3}$ instead of $\text{mol}\cdot\text{m}^{-2}$ for Γ . Even if Γ' is introduced in the model, Γ will be used in the discussion and figures to respect the physical meaning.

D_{wall} is fixed at $4 \times 10^{-11} \text{ m}^2\cdot\text{sec}^{-1}$. It is verified that the diffusion coefficient D_{wall} of the wall insures a uniform concentration Γ' in the direction normal to the surface at any time during the

calculation in a range of values from 4×10^{-10} to $4 \times 10^{-12} \text{ m}^2 \cdot \text{sec}^{-1}$, due to the small thickness of the active layer. Simulations were performed to check that, within this range, variations don't occur in the bulk and surface concentration profiles.

The global forms of the local equations (SI1) and (SI2) are here described using the Galerkin formulation (multiplication by a projective function α_p and integration on the domain of study, Ω), where $C_i = C, \Gamma'$ for $i = 1, 2$ respectively. The term A_i corresponds to the 2nd terms of eq. (SI1-2) defined only in the wall region:

$$\iint_{\Omega} \alpha_p \left[\frac{\partial C_i}{\partial t} + \nabla \cdot (-D_i \nabla C_i + \mathbf{V} C_i) - A_i \right] d\Omega = 0 \quad (\text{SI3})$$

The convection term is derived by taking into account the continuity equation $\nabla \cdot \mathbf{V} = 0$. By decomposing the product between α_p and the divergence, the second order derivative of (SI3) (divergence of the gradient) becomes:

$$\alpha_p \nabla \cdot (-D_i \nabla C_i) = \nabla \cdot (-\alpha_p D_i \nabla C_i) + D_i \nabla \alpha_p \cdot \nabla C_i \quad (\text{SI4})$$

Applying (SI4) in (SI3) and using the Ostrogradsky theorem, the divergence term is rejected at the external boundaries of the domain where it expresses the diffusion boundary condition of each species (here equal to zero, *i.e.* no diffusion flux at the external boundaries of the domain).

$$\iint_{\Omega} \left[\alpha_p \frac{\partial C}{\partial t} + D \nabla \alpha_p \cdot \nabla C + \alpha_p \mathbf{V} \cdot \nabla C + \alpha_p k_{\text{on}} \Gamma'_{\text{max}} C - \alpha_p k_{\text{on}} \Gamma' C - k_{\text{off}} \Gamma' \right] d\Omega = 0 \quad (\text{SI5})$$

$$\iint_{\Omega} \left[\alpha_p \frac{\partial \Gamma'}{\partial t} + D_{\text{wall}} \nabla \alpha_p \cdot \nabla \Gamma' - \alpha_p k_{\text{on}} \Gamma'_{\text{max}} C + \alpha_p k_{\text{on}} \Gamma' C + k_{\text{off}} \Gamma' \right] d\Omega = 0 \quad (\text{SI6})$$

Numerical technique.

The finite element formulation is implemented in the software Flux-Expert® (Astek Rhône-Alpes, France)⁴ that is performed on a Silicon Graphics Octane 2 Unix workstation. The calculations are performed in the 2-D geometry described on Fig. SI1(a). The typical mesh size ranges from 2 to 10 μm as shown in Fig. SI1(b). The active layer is 1 mesh thick. For the continuous flow, the initial conditions are $C = 0$ in the channel and $\Gamma = 0$ in the wall. For the zero-flow calculations (*i.e.* in the “stop-flow” process), the initial Γ value of each step n is equal to the value of Γ at equilibrium reached at the step $n-1$. The physical boundary condition (9-paper) being introduced as a consumption term, the only numerical boundary conditions of the model are the Dirichlet conditions at the inlet ($C = C^0$ for $x = 0$) and the Neumann homogeneous conditions at the external walls ($\partial C/\partial n = \partial \Gamma/\partial n = 0$ for $y = -\delta$ or $y = h$ or $x = L$).

For the pressure driven (PDF) flow, a Poiseuille parabolic profile has been imposed, while for the electro-osmotic (EOF) flow, a uniform velocity profile has been imposed. For the “stop-flow” simulations, the velocity is set to zero in the entire domain. The typical Courant-Friederich-Levy (CFL) number $V \cdot \Delta t / \Delta x$ is 0.5, as the velocity imposed is $100 \mu\text{m} \cdot \text{sec}^{-1}$, the characteristic time step Δt is 10^{-2} sec and the local cell Δx size is $2 \mu\text{m}$.

Results and discussions

Effects of the velocity profile, diffusion coefficient and channel length on the adsorption.

Although pressure driven PDF flow is mainly used in fluidic immunoassays or for modeling adsorption kinetics in flow cells,^{5,6} EOF flow can also be used,⁷ for instance when the test involves capillary electrophoresis,⁸ or the electrophoretic separation of the free antibody and the antibody-antigen complex.⁹ A comparison between PDF and EOF flows is shown in Fig. SI2 as a function of D (diffusion limited regime). Diffusion coefficients vary between $3 \times 10^{-12} \text{ m}^2 \cdot \text{sec}^{-1}$, typical of big proteins like collagen and IgMs, to $3 \times 10^{-10} \text{ m}^2 \cdot \text{sec}^{-1}$, which is found for small proteins like insulin. $\Gamma/\Gamma_{\text{max}}$ distribution is reported at 6 seconds. The case of an IgG antibody is also presented ($D = 4 \times 10^{-11} \text{ m}^2 \cdot \text{sec}^{-1}$).

For the same mean velocity, the EOF flow gives a higher adsorbed concentration in the first part of the channel because, due to the uniform profile, the near wall analyte arrives more rapidly than with PDF flow. On the other hand, in the second part of the channel, where the front of the plug is, the wall concentration increases more rapidly for the PDF flow due to the faster velocity of the middle channel species ($V_{\text{max}} = 3/2 \bar{V}$).

For both flow types, the coverage increases with the diffusion coefficient, leading to similar concentration profiles for high D values ($D = 3 \cdot 10^{-10} \text{ m}^2 \cdot \text{sec}^{-1}$, corresponding to a transversal Peclet number $Pe_h = \bar{V} \cdot h/D = 16$). Indeed, at high D values, the differences between the flow profiles are damped by molecular diffusion. When D is very low ($Pe_h = 1.6 \times 10^3$), the wall concentration at 6 sec decreases rapidly along the channel. This dispersion of the profiles in function of D is particularly marked for the PDF flow, for which the middle channel species do

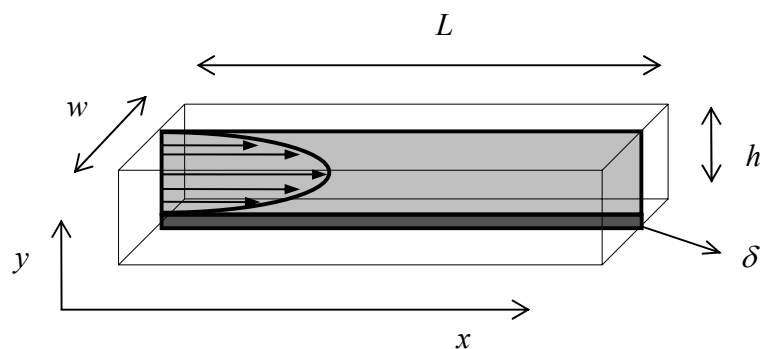
not have time to diffuse to the wall (they are wasted due to their higher velocity). Only the near wall analyte can contribute to the adsorption, but it is rapidly consumed because of its lower local velocity.

In order to check the valid range for extrapolating the results to longer channels, the effect of the channel length L has been studied for a constant residence time (by adapting the flow velocity proportionally to L). Fig. S13 shows the longitudinal distribution of Γ versus the dimensionless length of the channel x/L , for different velocities \bar{V} and channel lengths L . For velocity values below $10 \mu\text{m}\cdot\text{sec}^{-1}$, the Γ distribution is different, due to the competitive contribution of the longitudinal diffusion ($D/\delta_{\text{diff}} \sim 10 \mu\text{m}\cdot\text{sec}^{-1}$ corresponds to $\delta_{\text{diff}} \sim 4.2 \mu\text{m}$, where δ_{diff} is the typical 1-D diffusion length). For \bar{V} values higher than $50 \mu\text{m}\cdot\text{sec}^{-1}$, the plots are similar, whatever the couple (L, \bar{V}) . Consequently, the results of the previous figures can be applied, for example, to 1 cm channels (instead of 1 mm) with ten times higher flow rates (*i.e.* $1 \text{ mm}\cdot\text{sec}^{-1}$), *i.e.* conditions that are generally used experimentally.

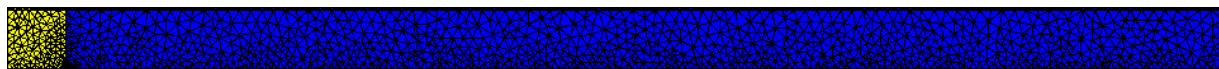
Time comparison between continuous flow and “stop-flow” in a diffusion limited case.

In order to see which procedure is faster, the continuous flow and the “stop-flow” are compared in Fig. SI4 in function of the absolute time. With $\bar{V} = 100 \mu\text{m}\cdot\text{sec}^{-1}$ the flow leads to the $\Gamma_{\text{eq}}^{\text{theor}}$ value in about the same time as the “stop-flow” mode (60 sec. instead of 70 sec. for the 99% of $\Gamma_{\text{eq}}^{\text{theor}}$). With $\bar{V} = 30 \mu\text{m}\cdot\text{sec}^{-1}$ the time to reach the full coverage is doubled (120 sec. for the 99% of $\Gamma_{\text{eq}}^{\text{theor}}$). As a consequence, for the same amount of analyte solution used, the “stop-flow” is faster than the continuous flow.

- (1) Reinmuth, W. H. *Journal of Physical Chemistry* **1961**, *65*, 473-&.
- (2) Delahay, P.; Trachtenberg, I. *Journal of the American Chemical Society* **1957**, *79*, 2355-2362.
- (3) Lionello, A.; Josserand, J.; Jensen, H.; Girault, H. H. *Lab on a Chip* **2005**, *5*, 254-260.
- (4) Astek Rhône-Alpes: 1 place du Verseau, 38130 Echirolles, France.
- (5) Mason, T.; Pineda, A. R.; Wofsy, C.; Goldstein, B. *Mathematical Biosciences* **1999**, *159*, 123-144.
- (6) Filippov, L. K.; Filippova, N. L. *Journal of Colloid and Interface Science* **1997**, *189*, 1-16.
- (7) Dodge, A.; Fluri, K.; Verpoorte, E.; de Rooij, N. F. *Analytical Chemistry* **2001**, *73*, 3400-3409.
- (8) Cheng, S. B.; Skinner, C. D.; Taylor, J.; Attiya, S.; Lee, W. E.; Picelli, G.; Harrison, D. J. *Analytical Chemistry* **2001**, *73*, 1472-1479.
- (9) Wang, J.; Ibanez, A.; Chatrathi, M. P.; Escarpa, A. *Analytical Chemistry* **2001**, *73*, 5323-5327.



(a)



(b)

Figure S11. (a) Scheme of the model, where the diffusion coefficient of the analyte D is defined in the light gray bulk region (of height h), while the number of active sites Γ_{\max} , the wall diffusion coefficient to insure a uniform coverage D' , the forward and reverse rates of adsorption k_{on} and k_{off} are defined at the interface. Dimensions are: $h = 50 \mu\text{m}$; $\delta = 2 \mu\text{m}$; $L = 1 \text{mm}$ (figure not in scale). The analyte solution runs in the channel with a pressure driven flow (PDF) profile with a mean velocity \bar{V} . (b) Mesh used for the simulations. The typical mesh size ranges from $2 \mu\text{m}$ for the active layer on the bottom to $10 \mu\text{m}$ on the top of the channel.

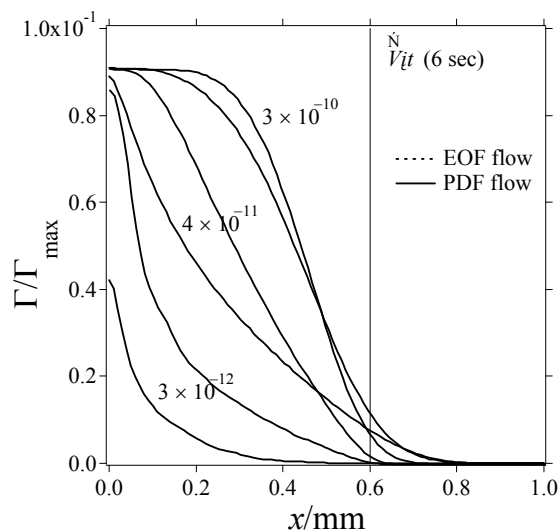


Figure SI2. Comparison between EOF flow and PDF flow, and effect of the analyte diffusion coefficient on the adsorption. Plots represent Γ/Γ_{\max} profiles versus x , at 6 sec from the beginning of pumping. $\Gamma_{\max} = 10^{-9} \text{ mol}\cdot\text{m}^{-2}$, $K = 10^4 \text{ m}^3\cdot\text{mol}^{-1}$, $C^{\circ} = 10^{-5} \text{ mol}\cdot\text{m}^{-3}$, $\bar{V} = 100 \mu\text{m}\cdot\text{sec}^{-1}$. As $\psi = 0.1$, $\Gamma_{\text{eq}}^{\text{theor}}/\Gamma_{\max} = 9.1 \times 10^{-2}$, $k_{\text{off}} = 100 \text{ sec}^{-1}$ (the adsorption is diffusion limited). D varies between $3 \times 10^{-12} \text{ m}^2\cdot\text{sec}^{-1}$ and $3 \times 10^{-10} \text{ m}^2\cdot\text{sec}^{-1}$ and the Peclet number varies between 3.33×10^5 and 3.33×10^2 respectively. The vertical line represents the distance run by the solution if no diffusion occurred.

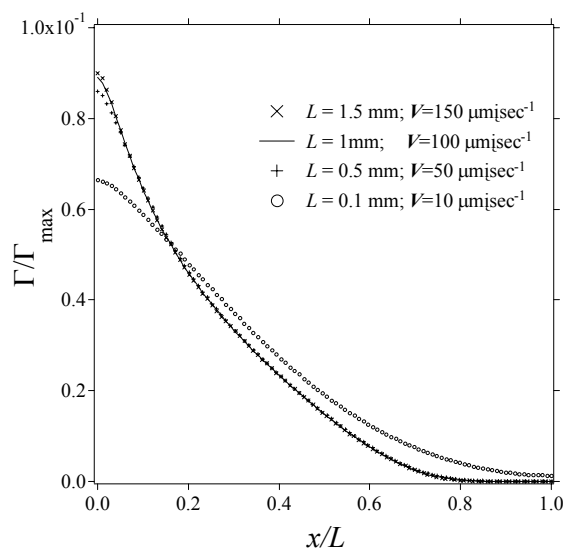


Figure SI3. Comparison of results for different couples (\bar{V}, L) (*i.e.* flow velocity and channel length). Plots represent Γ/Γ_{\max} in function of the normalised distance x/L . $\bar{V} = 150, 100, 50$ and $10 \mu\text{m}\cdot\text{sec}^{-1}$ for $L = 1.5, 1, 0.5, 0.1$ mm respectively. $D = 4 \times 10^{-11} \text{m}^2\cdot\text{sec}^{-1}$. The other parameters are those of Fig. SI2.

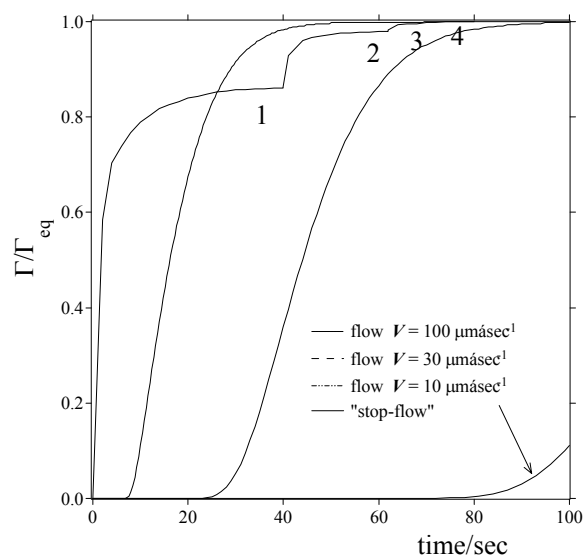


Figure SI4. The results of Fig. 5a are here presented versus the absolute time. $D = 4 \times 10^{-11}$

$\text{m}^2\cdot\text{sec}^{-1}$, $\Gamma_{\text{max}} = 10^{-9} \text{ mol}\cdot\text{m}^{-2}$, $K = 10^4 \text{ m}^3\cdot\text{mol}^{-1}$, $C^{\circ} = 10^{-5} \text{ mol}\cdot\text{m}^{-3}$.